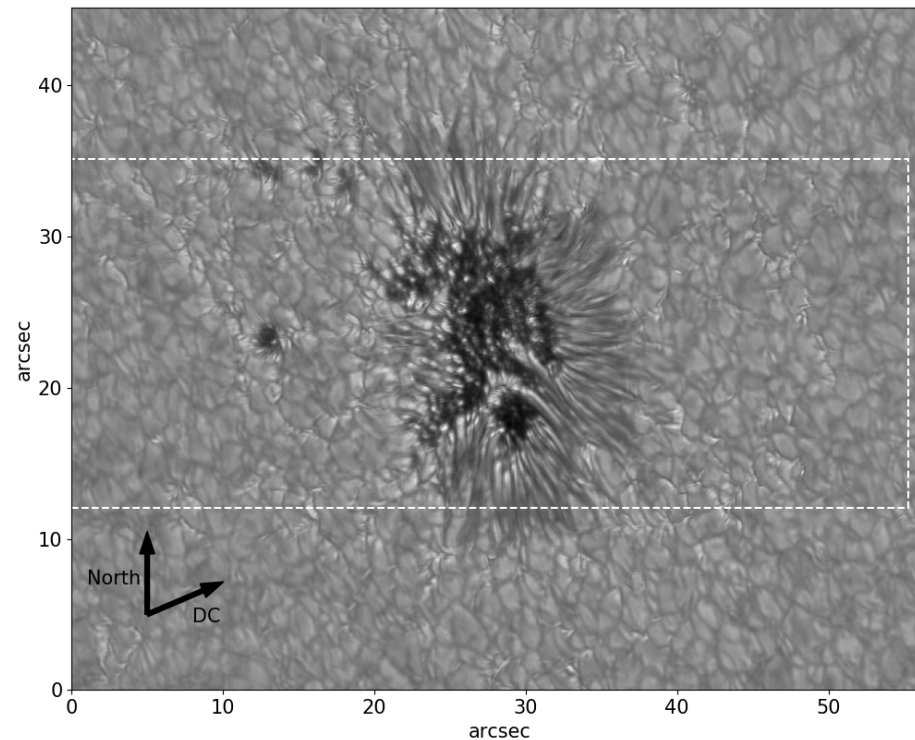


The role of the chromospheric canopy in the formation of a penumbra

Philip Lindner

Affiliation: Leibniz-Institut für Sonnenphysik (KIS)



Publication:

Astronomy & Astrophysics, Volume
673, id.A64, 15 pp.

Collaborators:

Christoph Kuckein
Sergio Gonzalez Manrique
Nazaret Bello González
Lucia Kleint
Thomas Berkefeld

GREGOR TiO image from 2020/10/16

SOLARNET Conference Potsdam 8-12 May 2023

09.05.2022

1. Introduction

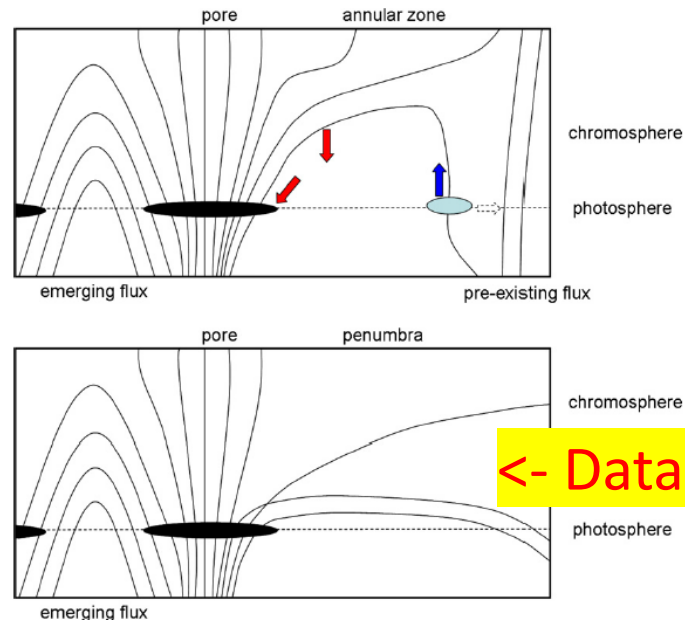
Conditions for penumbra formation:

- **Magnetic flux threshold** of $3 \cdot 10^{20}$ Mx (Keppens & Martinez Pillet, 1996). Transition region also possible (Tlatov & Pevtsov 2014; Cho et al. 2015)
- **Hints for chromospheric canopy:**
 - Observations: Shimizu et al. 2012 observed annular zone (3''-5'') in chromospheric Ca II H core intensity images before penumbra formation. Also Murabito et al. 2021: Special case
 - Simulations: Rempel 2012 found that a penumbra only forms when the magnetic fields at the top of the simulation box are forced to be horizontal ($\alpha > 1$).
 - Lack of data to verify the connection.
- **Additional conditions?**

Penumbra formation scenarios (origin of inclined fields)

Top-down scenario

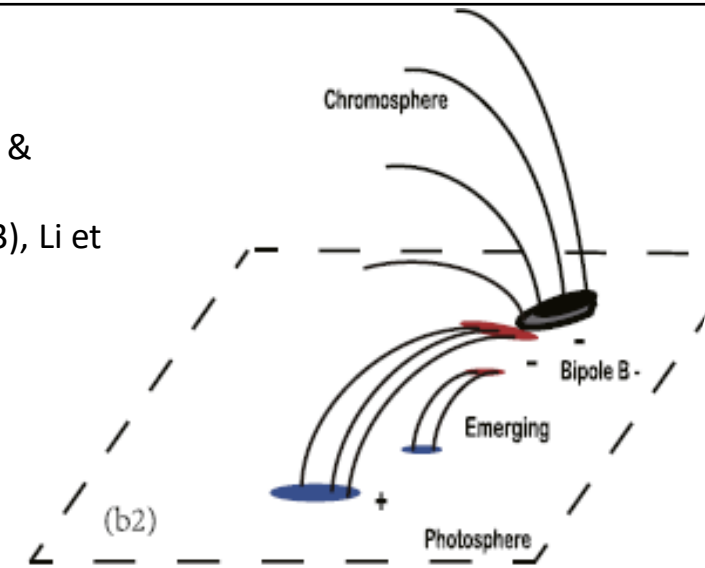
- First formulated by Wentzel 1992
- See also: Shimizu et al. 2012, Romano et al. 2014, Murabito et al. 2016



Adapted from
Romano et al. 2014

Bottom-up scenario

- First formulated by Leka & Skumanich (1998),
- See also: Lim et al. (2013), Li et al. (2018, 2019). Also Zuccarello et al. (2014)



Adapted from Li et al. 2019

<- Data missing ->

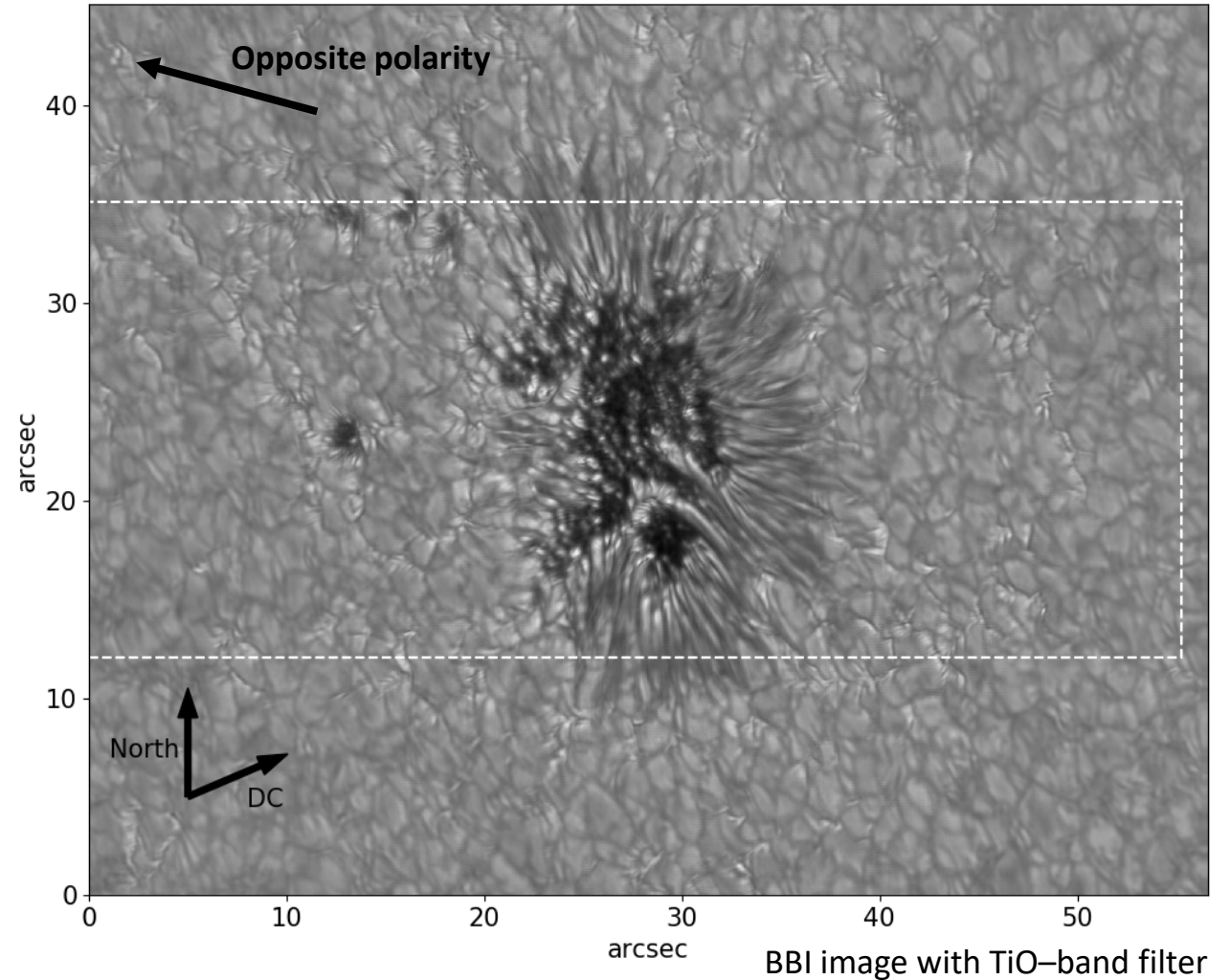
2. GREGOR Data overview

Observations with GREGOR telescope

- Target: sunspot with partial penumbra (NOAA 12776)
- Date: 2020 / 10 / 16 (Gregor Science verification phase)
- $\mu = 0.64$
- HMI data: Sunspot just formed and stays in this configuration for several days

Instruments:

- **BBI** imaging: G-band (431 nm) & TiO-band (706 nm) filters
- **GRIS** slit-spectropolarimetry in 10830 Å region
 - Ca I 10839 Å line (low photosphere)
 - Si I 10827 Å line (mid-high photosphere)
 - He I 10830 Å triplet (high chromosphere)



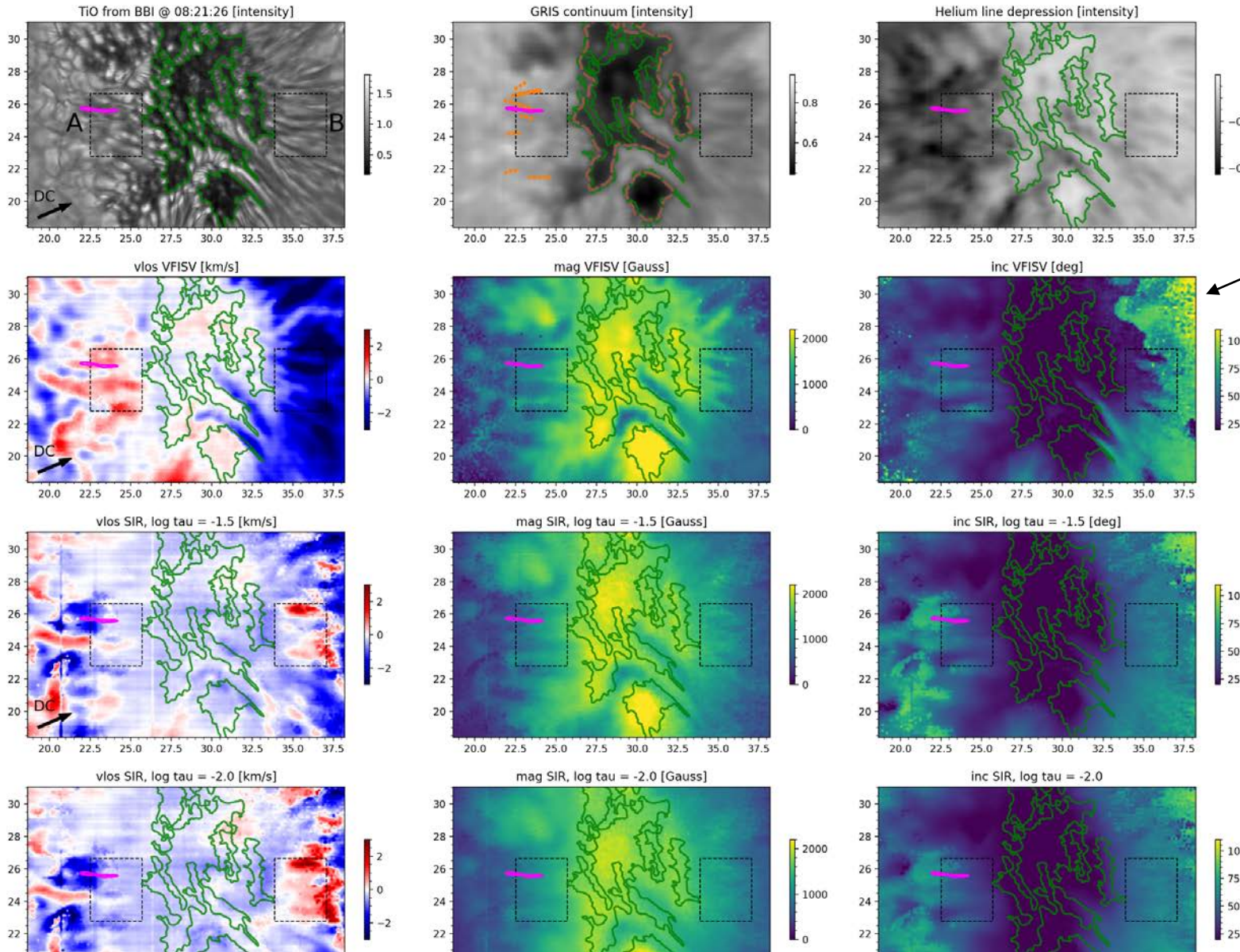
3. GRIS data: Magnetic field throughout atmosphere

Separate inversions

- Ca I 10839 Å line: **VFISV** (Borrero et al. 2011)
- Si I 10827 Å line: **SIR** (Ruiz Cobo & del Toro Iniesta 1992), height-dependent
- He I 10830 Å: **HAZEL** (Asensio Ramos et al. 2008)

First plausibility check:

- Penumbral filamentary structure dissolves towards higher layers
- Evershed flow is also only clearly visible in low photosphere

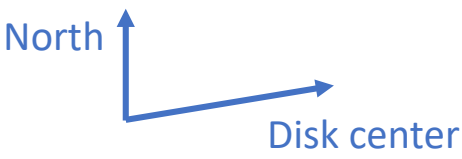


Local reference frame!

Ca I 10839 Å

Si I 10827 Å

Si I 10827 Å



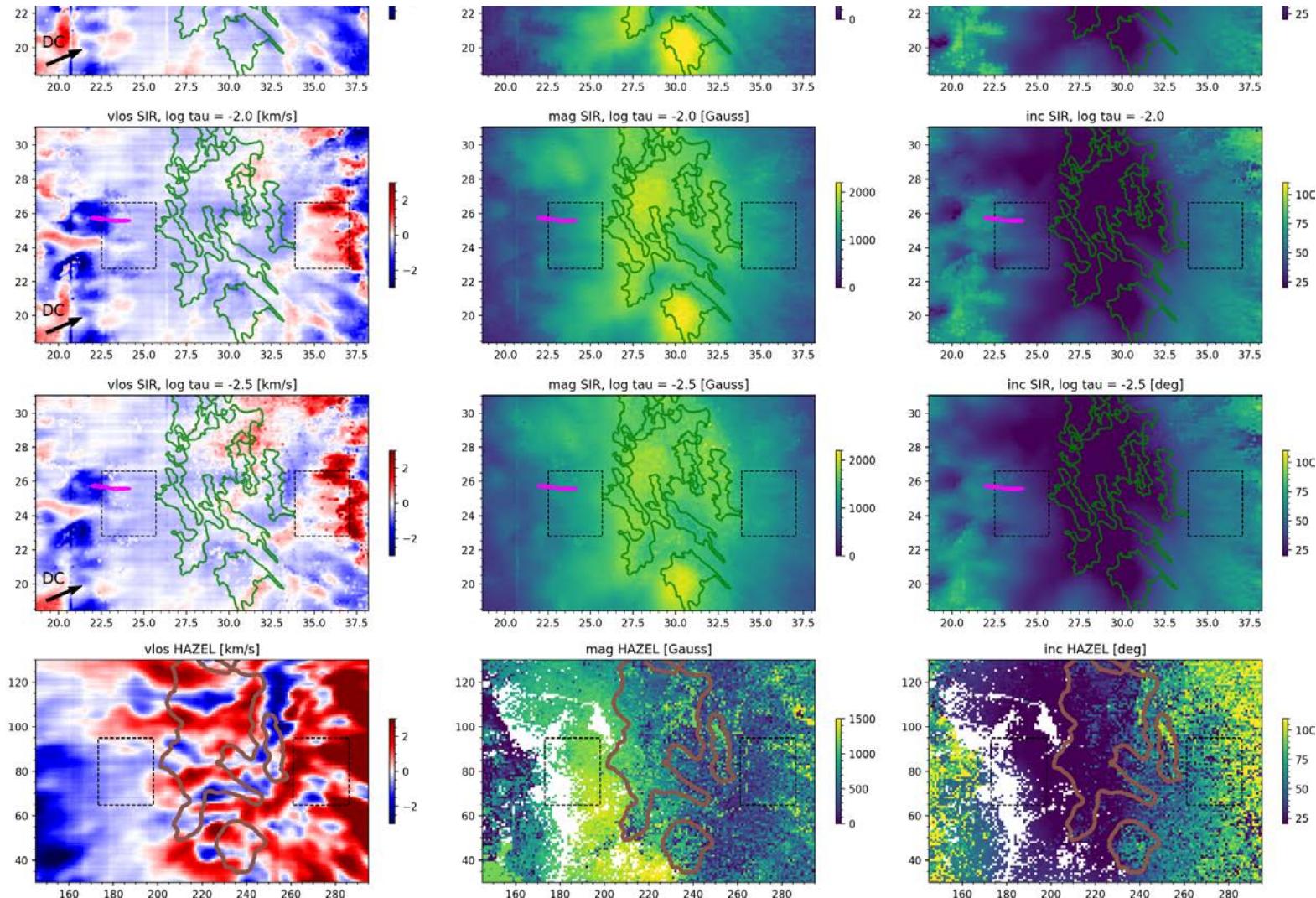
3. GRIS data: Magnetic field throughout atmosphere

Separate inversions

- Ca I 10839 Å line: **VFISV** (Borrero et al. 2011)
- Si I 10827 Å line: **SIR** (Ruiz Cobo & del Toro Iniesta 1992), height-dependent
- He I 10830 Å: **HAZEL** (Asensio Ramos et al. 2008)

First plausibility check:

- Penumbral filamentary structure dissolves towards higher layers
- Evershed flow is also only clearly visible in low photosphere

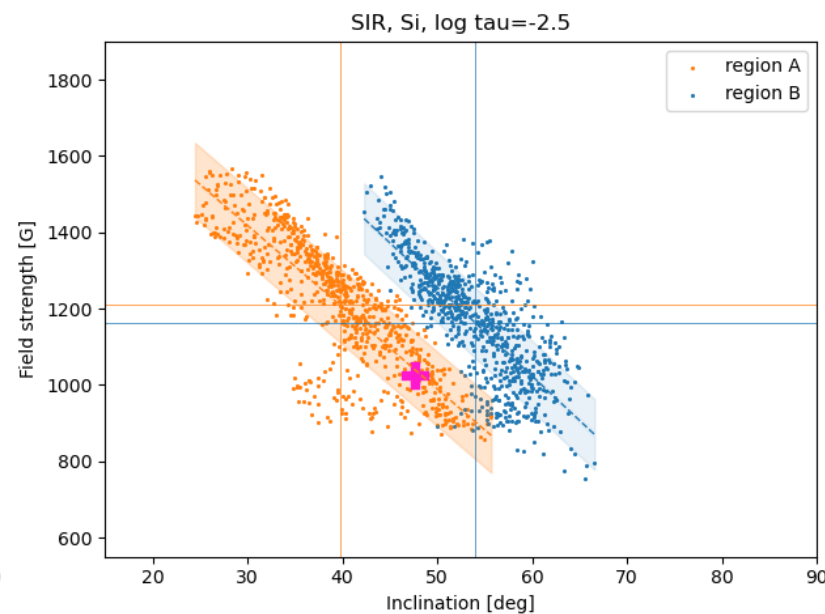
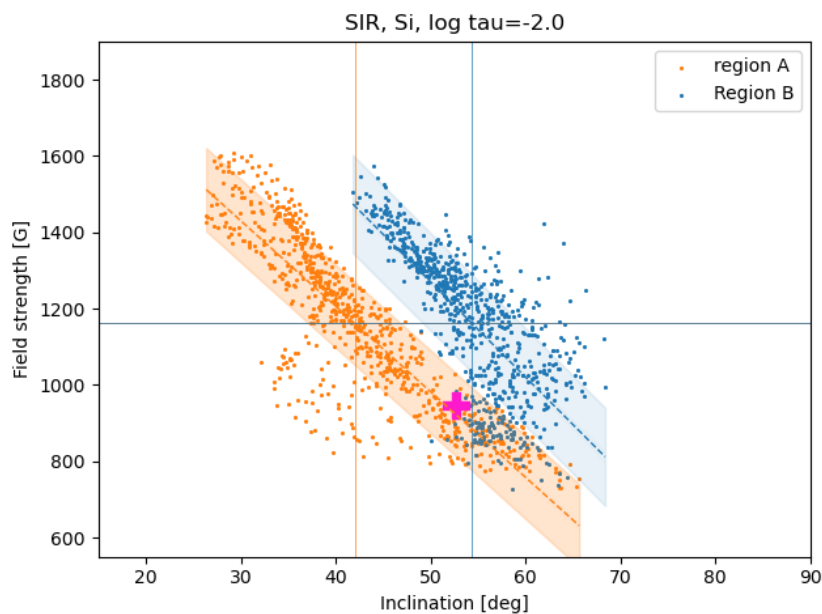
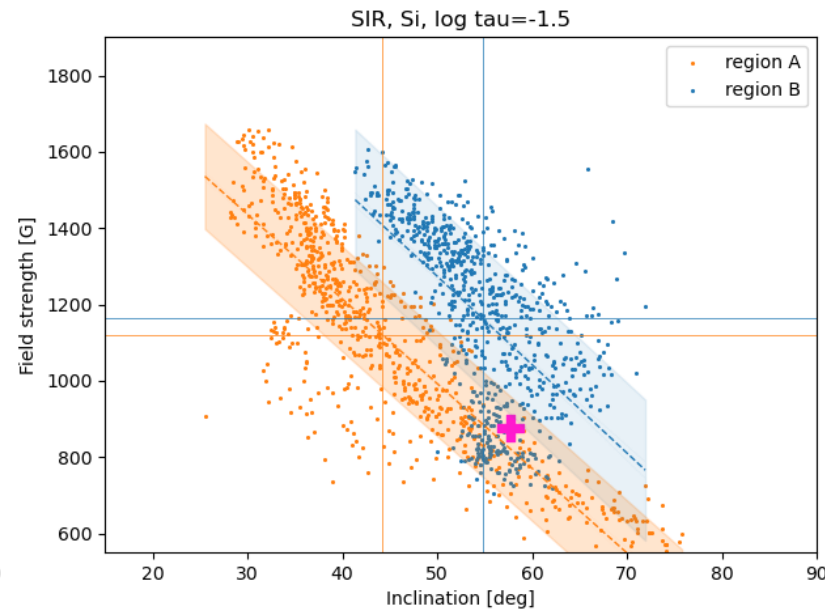
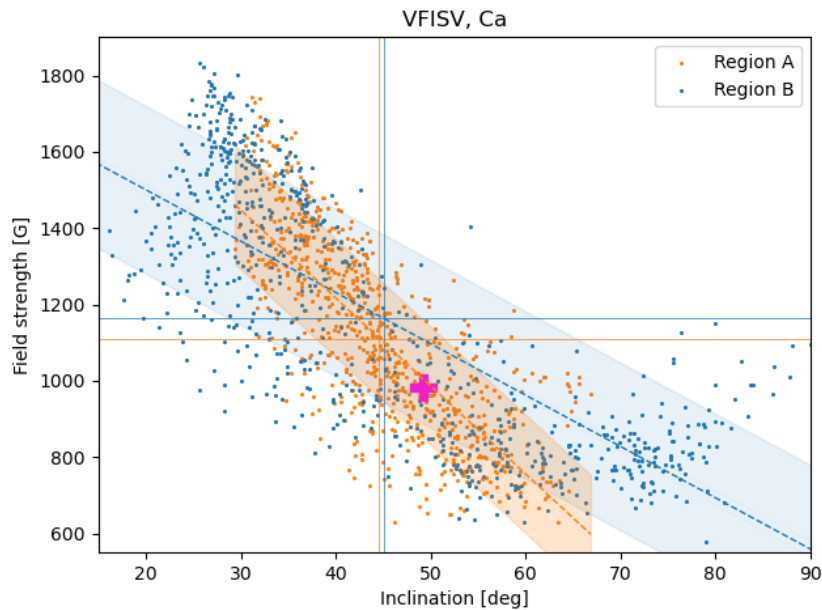


Si I 10827 Å

Si I 10827 Å

He I 10830 Å triplet

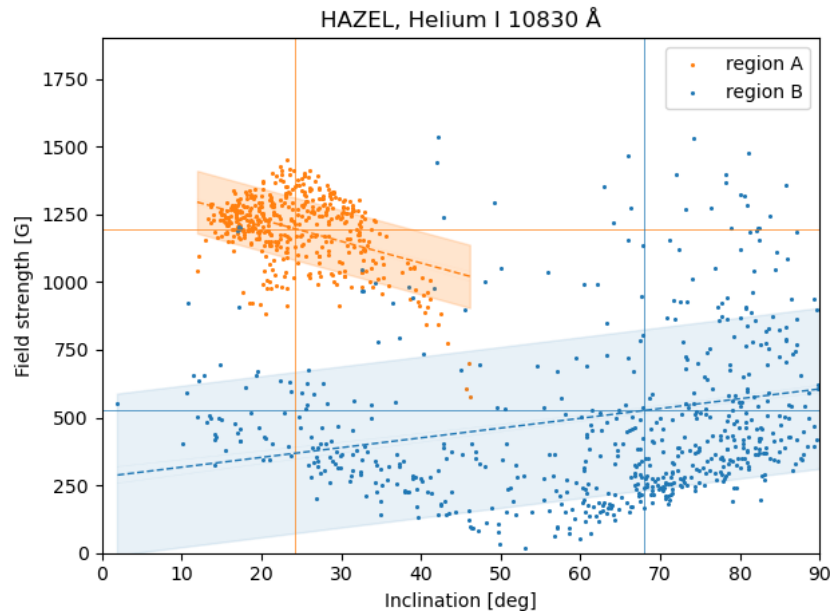
3. GRIS data: Magnetic field throughout atmosphere



region A: no penumbra
region B: with penumbra

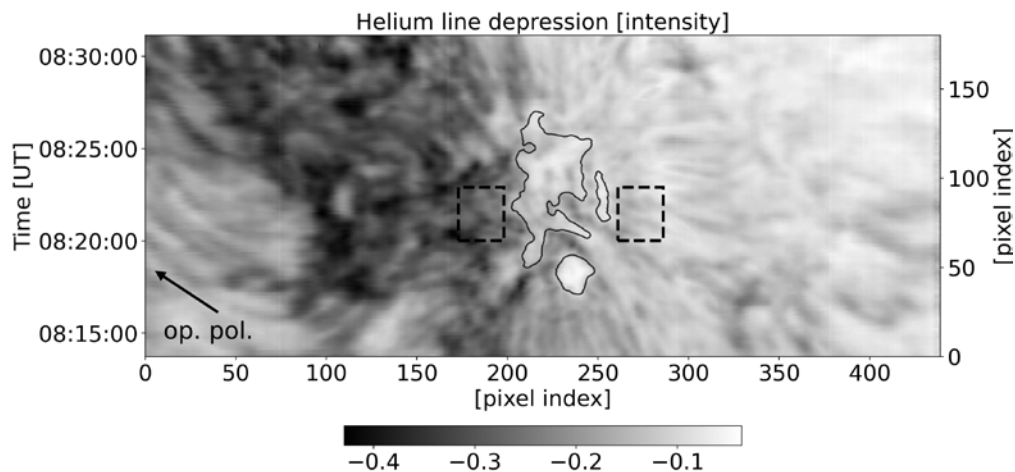
- Overlap between the distributions of region A and region B in the deep photosphere.
- Differences of distributions increase with height
- Average field inclination is similar between A and B in deep photosphere only.

3. GRIS data: Magnetic field throughout atmosphere



Region A: no penumbra
Region B: with penumbra

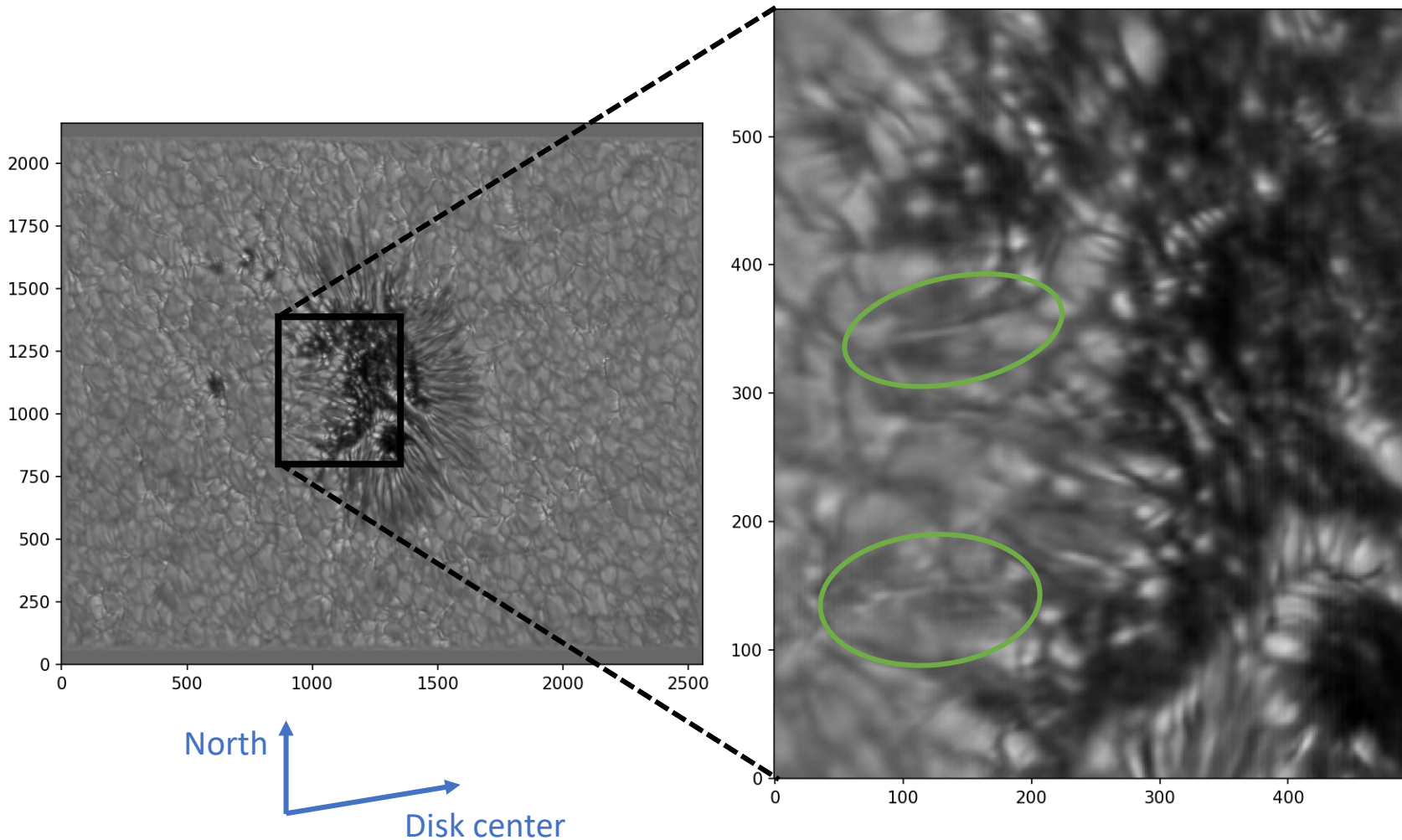
- Region A: Inversion problems with 39 % of the pixels (low circular, high linear polarization)
- Region A: close to vertical fields
- Region B: close to horizontal field



- Large dark area seen in Full-scan map
-> distortion of chromospheric canopy

5. BBI high-resolution data: Thin bright filaments

sd-2020-10-16T08:12:09.432_tc.fts / TiO



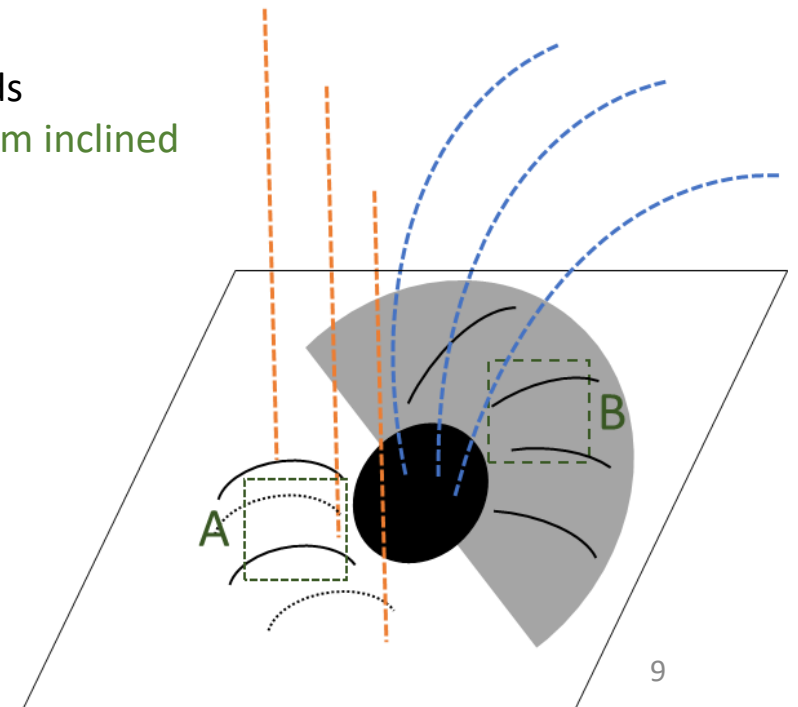
- Thin, straight filaments seen with high contrast in TiO filter images
- “Thin Bright Filaments” (TBFs):
 - **Maximum width:** 0.1 arcsec (diffraction limit of the telescope)
 - **Average lifetime:** 4 minutes
 - **Average length:** 1.4 arcsec
- Not resolved in GRIS data

6. Conclusions and discussion points

- Magnetic topologies in region A (no penumbra, TBFs) and region B (penumbra) are similar in the deep photosphere.
 - It is surprising that, without a continuum image, one would not be able to tell from magnetic field maps whether a penumbra is present or not!
- Differences in field topology between region A and region B are present in higher layers. Largest difference in chromosphere. Dark structure in Helium line depression maps
 - Something must prevent the penumbra from forming in region A. The deep photospheric magnetic topology is similar ('ingredients' for formation are given). -> Hint toward the disturbed chromospheric canopy being the reason. This is the first evidence of the connectivity between the photosphere and chromosphere playing a role in penumbra formation based on spectropolarimetric data from both the photosphere and the chromosphere.
- Region A: Close-to-vertical chromospheric, but inclined photospheric (stable) magnetic fields
 - Unlikely that inclined photospheric field originate from chromosphere -> Originate from inclined emerging magnetic fields ("bottom-up")

Proposed bottom-up scenario for this sunspot: Magnetic flux tubes with inclined fields emerge from below the surface.

- In region A, the chromospheric canopy is disturbed and the inclined fields are not kept stably. These unstable flux tubes are seen as TBFs, which escape into higher layers or dissolve.
- In the remaining regions, an intact canopy exists, which 'traps' the photospheric fields and a penumbra can form.



References

- Lindner, P., Kuckein, C., Gonzalez Manrique, S. J., et al. 2023, A&A, 673, A64
- Keppens, R. & Martinez Pillet, V. 1996, A&A, 316, 229
- Tlatov, A. G. & Pevtsov, A. A. 2014, Sol. Phys., 289, 1143
- Cho, I. H., Cho, K. S., Bong, S. C., et al. 2015, ApJ, 811, 49
- Murabito, M., Guglielmino, S. L., Ermolli, I., et al. 2021, A&A, 653, A93
- Wentzel, D. G. 1992, ApJ, 388, 211
- Shimizu, T., Ichimoto, K., & Suematsu, Y. 2012, ApJ, 747, L18
- Romano, P., Guglielmino, S. L., Cristaldi, A., et al. 2014, ApJ, 784, 10
- Murabito, M., Romano, P., Guglielmino, S. L., Zuccarello, F., & Solanki, S. K. 1062016, ApJ, 825, 75
- Leka, K. D., & Skumanich, A. 1998, ApJ, 507, 454
- Lim, E.-K., Yurchyshyn, V., Goode, P., & Cho, K.-S. 2013, ApJ, 769, L18
- Li, Q., Yan, X., Wang, J., et al. 2018, ApJ, 857, 21 92
- Li, Q., Yan, X., Wang, J., et al. 2019, ApJ, 886, 149 93
- Zuccarello, F., Guglielmino, S. L., & Romano, P. 2014, ApJ, 787, 57